

## Research Article

# Advancements in Aerogels for Aerospace Applications: A Comprehensive Review

*Aditya Sehgal*

Student, Mechanical Department Park College of Engineering and Technolog.

## I N F O

**E-mail Id:**

sehgaladi8@gmail.com

**Orcid Id:**

<https://orcid.org/0009-0002-4059-2648>

**How to cite this article:**

Sehgal A. Advancements in Aerogels for Aerospace Applications: A Comprehensive Review *J Adv Res Aero Space Sci* 2023; 10(1): 12-26.

Date of Submission: 2022-02-10

Date of Acceptance: 2022-03-16

## A B S T R A C T

**Abstract:**

Aerogels are made using the sol-gel method and supercritical drying technology. They are very porous structures. When compared to other solids, silica aerogel has the lowest density, thermal conductivity, refractive index, and dielectric constant of all the different types of aerogels. Its acoustical properties let sound waves to be absorbed, slowing them down to 100 m/s from 332 m/s for air. The outcome is hardly what was anticipated when it comes to commercialization, though. It seems that mass production, particularly in the aerospace industry, has dawdled behind. This paper highlights the evolution of aerogels in general and discusses the functions and significances of silica aerogel in previous astronomical applications. Future outer-space applications have been proposed as per the current research trend. Finally, the implementation of conventional silica aerogel in aeronautics is argued with an alternative known as Maerogel.

**Keywords:** Optics, Chemistry, Acoustic Insulation, Kinetic Energy Absorption, Electronics

## Introduction

Aerogels are nanoporous light materials made up of an open-cell network that have a number of unique properties that pique the interest of researchers in many different fields of science and technology. Their list of potential uses is practically endless, spanning fields like thermal and acoustic insulation, kinetic energy absorption, electronics, optics, chemistry, and biomedicine.<sup>1,5</sup> The most intriguing properties among the different types of aerogels are those of silica aerogel, which is the porous nanostructured form of silica dioxide. These properties include hydrophobicity, low sound velocity (100 m/s), low refractive index (1.05), low dielectric constant (1.0-2.0), low thermal conductivity (0.015 W/mK), low bulk density (0.1 g/cm<sup>3</sup>), and optical transparency in the visible spectrum (99%). Due to the presence of nanosized pores in their microstructure, they exhibit this distinct combination of qualities.

Over the past two decades, numerous papers have explored the scientific understanding of silica aerogel and its thermal behavior. Despite NASA's use in astronaut missions, silica aerogel remains primarily used for scientific purposes. The aviation industry could be a promising market niche for high-performance thermal insulation materials. However, there is no literature discussing commercialization of silica aerogel in the aerospace sector. Future outer-space applications are proposed based on current research trends, and an alternative called Maerogel is argued for<sup>9,3</sup>

Aerogel, also known as "blue smoke" or "frozen smoke" due to its cloudy appearance (see Figure 1), is a long-forgotten substance that Samuel Stephens Kistler created while he was a student at the College of the Pacific in Stockton, California, in the United States. Despite appearing to be a recent invention of nanotechnology due to its features of nanostructure. He published the first article on aerogels



**Figure 1. Matches on aerogel over a flame.<sup>17</sup>**

in nature in 1931<sup>14</sup>, defining an aerogel as a gel in which the liquid phase has been replaced by a gas in a way that preserves the solid network with little to no gel shrinkage. The effectiveness of this procedure was dependent on a crucial step known as supercritical drying, which involved heating the gel system in an autoclave above the critical pressures and temperatures of the gel's liquid phase. After allowing the supercritical fluid to form to escape, a very porous and low-density substance was left behind.

Kistler created the first aerogel utilising sodium silicate (water-glass) as the silica precursor. Over time, he created organic and metal oxide aerogels out of rubber, cellulose, nitrocellulose, gelatin, agar, tungsten oxide, ferric oxide, tin oxide, nickel tartrate, and other materials.<sup>15</sup> He expanded his research into the silica aerogel's physical characteristics by adding gases including air, carbon dioxide, and chlorofluorocarbon, while focusing on its structure, density, and thermal conductivity.<sup>16</sup> Thus, silica aerogel was shown to have the lowest heat conductivity of any solid at atmospheric pressure.<sup>18</sup> In the 1950s, one of Kistler's patents was given to Monsanto Corporation for the aim of mass producing silica aerogels for uses such as thickening agents and thermal materials.<sup>19</sup> He later developed the first hydrophobic silica aerogels via silylation utilising trichloromethylsilane in order to produce water repellents.<sup>20</sup>

Unexpectedly, Masanto's research was abruptly put on hold when a very affordable fumed silica procedure utilising tetrachloride was introduced in the 1960s, ending all production. Since then, there has been no interest in aerogels because of the laborious and drawn-out processes required for their synthesis, as well as their expensive production. Commercialization took a very long time as a result, until a team of scientists led by Teichner and Nicolao

in France reformulated a simpler preparation in 1968 by using the sol-gel chemistry to prepare silica aerogel in place of the waterglass used by Kistler. This new formulation used tetramethyl orthosilicate (TMOS), an alkoxy silane, which was then removed under supercritical conditions.<sup>21</sup> Magnesium oxide (MgO), alumina (Al<sub>2</sub>O<sub>3</sub>), titania (TiO<sub>2</sub>), zirconia (ZrO<sub>2</sub>), silica (SiO<sub>2</sub>), and mixtures of ZrO<sub>2</sub>-MgO, Al<sub>2</sub>O<sub>3</sub>-MgO, and TiO<sub>2</sub>-MgO were created into aerogels. When going that approach, it was found that these aerogel oxides had greater textural characteristic values than those created utilising the original technique.

Additionally, the surface area was larger than that of their equivalent pure oxide aerogels.<sup>22</sup> This achievement set off a new revolution in science and technology, which led to in-depth research on this nanotechnology material. Aerogels were used for the first time in science when Cantin et al. created the Cherenkov radiation detector in 1974. In order to outfit the TASSO Cherenkov detector, mass manufacture of monolithic, very transparent silica aerogel tiles was subsequently initiated.<sup>23</sup>

The first plant to use TMOS to create blocks of silica aerogel was built in Sweden, but it was destroyed by an explosion in 1984 caused by a leak in the autoclave when methanol was present. Airglass Corporation refurbished the facility and is now in charge of running it.<sup>24</sup> The hazardous nature of TMOS made it necessary to replace it. Tewari and Hunt at Berkeley soon discovered that tetraethyl orthosilicate (TEOS) was a safer reagent that would not affect the aerogels' quality.<sup>25</sup>

### **However, the method was not yet secure enough for mass production.**

Hunt persisted in looking for ways to improve the process and came up with the concept of substituting liquid carbon dioxide for the alcohol in the gel before supercritical drying since CO<sub>2</sub> is inflammable and needs less heat and pressure to become supercritical.<sup>26</sup> This would lower any danger of hazards and boost energy efficiency, which would lower the cost of manufacturing. At the same time, BASF in Germany announced that it had created a second CO<sub>2</sub> replacement pathway using sodium silicate. Up until 1996<sup>4</sup>, they marketed the item under the name Basogel. The development of helium pycnometry in 1987 for determining the skeletal density of aerogels produced data showing that the density fluctuates with solvent content, pH, and heat treatment for densifying.<sup>27</sup> Pekala at LLNL broadened the types of aerogel during the end of the 1980s by employing the sol-gel process to create organic and carbon aerogels from the organic polymer resorcinolformaldehyde (RF).<sup>28</sup>

Using a two-step acid-base procedure that involves replacing the alcohol with an aprotic solvent by distillation, producing gelation, Tillotson and Hrubesh created monoliths of diaphanous silica aerogel with the lowest density, 0.003

g/cm<sup>3</sup>, and of porosity up to 99.8%.<sup>29</sup> That was the 1990s' first success with aerogel.

Since then, NASA has been employing tiles made of these aerogels for space exploration. Later, it was discovered that the polymer that makes up an RF aerogel is dehydrated, leaving behind an aerogel made of carbon when heated to temperatures of several hundred degrees Celsius in an inert atmosphere (such as nitrogen or argon). In contrast to silica aerogel, carbon aerogel is an electrical conductor. It was referred to as a "electrochemical doublecapacitor with high-power density and high-energy density" and given the name aerocapacitor.<sup>30,31</sup>

The subcritical drying technique, which was developed to create low-density silica aerogels for thermal insulation, was another significant advancement.<sup>32</sup> To avoid significant gel shrinkage during the quick drying at ambient pressure, the approach comprised a number of ageing and pore chemical modification phases. At atmospheric circumstances, the density fluctuates between 0.15 and 0.3 g/cm<sup>3</sup> and has a thermal conductivity of 0.02 W/mK.

The ambient pressure drying (APD) method was expanded by Prakash et al. to significantly reduce the cost of silica production. It was done using a straightforward dip-coating procedure that involved surface modification to cause reversible drying shrinkage.<sup>33</sup>

Waterglass served as a forerunner because of its low cost and inflammability. It was found that the resulting aerogel had a similar density and porosity to that produced by the supercritical drying method. Since then, numerous studies employing the APD approach describing the synthesis and physical characteristics of silica aerogel have been published, highlighting its benefits. However, due to the drawn-out process of washing and swapping solvents, the path changes and some techniques take longer than others.<sup>34,39</sup>

The rapid supercritical extraction (RSCE), which accelerated supercritical heating, came next. In an experiment conducted by John Poco at LLNL in 1996, the sol-gel was placed inside a pressurised mould in which the supercritical conditions were managed to prevent unneeded expansion and, as a result, cracking.<sup>40,41</sup> At the start of this millennium, significant improvement began. As long as the relevant metal ions have a valency of equal or more than +3 in their formation oxidation state, Gasch and Tillotson in 2001 discovered an easy, affordable, and efficient approach to create metal oxide aerogels. The outcomes seemed promising, and large-surface-area blocks of microporous materials were created.<sup>42</sup>

A year later, Leventis et al. treated silica aerogels using diisocyanates to create X-aerogels, which are extremely light mechanically modified aerogels. The latter's strength

was doubled by 300, whereas its specific compressive strength is around ten times more than that of steel.<sup>43</sup> In order to further broaden the applications of aerogels, his study was expanded with the aid of other researchers to look into the polymer cross-linking with different forms of aerogel, such as transition metal oxides and organics.<sup>44</sup> By adding a polymer as a conformal coating to the silica skeleton, X-aerogels have been created.

However, Mohanan et al. reported on semiconductors constructed of metal chalcogenide in 2005. They employed a technique that involved supercritical drying followed by the oxidation aggregation of metal chalcogenide nanoparticle building blocks. High porosity and surface area were present in the resultant semiconductor, and the typical quantumconfined optical characteristics were the same as those of the nanoparticle constituents.<sup>45</sup> Monolithic nanoporous metal foams, with exceptionally low densities and high surface areas of 0.011 g/cm<sup>3</sup> and 270m<sup>2</sup>/g, respectively, were created the next year.<sup>46</sup>

Iron, cobalt, copper, and silver were chosen as metals, however other probable ones are still being investigated. Then, in 2007, carbon nanotube aerogels were developed using a novel synthesis technique that included aqueous gel precursors, supercritical drying, and freeze drying. By doping polyvinyl alcohol, the nanotubes can be strengthened so that they can withstand 800 times more weight than their unmodified counterparts. They also function well as heat and electrical conductors.<sup>47</sup>

In her 2004 patent application and 2007 patent, Halimaton described how to make pure silica aerogel using the sol-gel process and supercritical CO<sub>2</sub> drying.

But she obtained the silica from rice husk ash (RHA), an agricultural waste product (see Figure 2). The brand name "Malaysian-made Aerogel" is known as "Maerogel" [48]. It has been demonstrated that the latter's texture and physical characteristics are comparable to those of conventional silica aerogels (see Table 1). A sodium silicate solution comprising 1 to 16% by weight of SiO<sub>2</sub> is created by first dissolving rice husk ash in aqueous sodium hydroxide at a Na<sub>2</sub>: SiO<sub>2</sub> ratio of 1: 3.33. The sodium silicate is subsequently changed into silica by adding concentrated sulfuric acid to the ensuing water-glass solution to create a silica hydrogel. The next step is ageing, which will allow the gel structure to form. This could last for up to forty days. To create an alcogel, the water is then replaced with a C1 to C4 alcohol, preferably methanol or ethanol. To create an aerogel, the latter is dried at supercritical conditions after alcohol is replaced with carbon dioxide. The alcogel and additional alcohol are placed in an autoclave with a thermocouple and temperature controller, and the temperature is gradually increased within the autoclave until the critical temperature and pressure are reached. This

is the preferred method for performing the supercritical extraction. For example, the temperature could be raised at a pace of 50°C per hour for the duration required to reach the critical temperature. After some time, the pressure and temperature are gradually brought down to atmospheric levels, allowing the alcohol vapour to be released through a controlled leak. Over the course of, say, twelve hours, the temperature may be lowered. The additional alcohol should be added until there is enough alcohol in the autoclave to attain the critical pressure.

The resulting aerogels have hydroxyl groups on their surface and are hydrophilic; however, these groups can be changed to alkoxy groups to make the aerogels hydrophobic. This may be accomplished, for instance, by vaporising methanol and sprinkling it over a heated aerogel sample. The methylation reaction is more successfully conducted in a closed system, where the sample can be placed in a tube that extends between a flask of boiling methanol and a condenser that is connected back to the flask, and is encased in an external furnace. The furnace may have a temperature of around 250 C. Preferably, the samples are outgassed for at least 15 hours before and after the methylation process at a temperature of about 100 °C and a decreased pressure of roughly 1.33 10<sup>5</sup> kPa.<sup>48</sup>

**Table I. Physical properties of conventional silica aerogel and Maerogel.**

Property	Conventional aerogel	Maerogel	Comments
Apparent density	0.003-0.35 g/cm <sup>3</sup>	0.03 g/cm <sup>3</sup>	Commonly ~0.1 g/cm <sup>3</sup> for conventional aerogels; Usually 0.03 g/cm <sup>3</sup> for Maerogel
Internal surface area	600-1000 m <sup>2</sup> /g	700-900 m <sup>2</sup> /g	
Mean pore diameter	20 nm	20.8 nm	Varies with density
Particle diameter	2-5 nm	5 nm	Determined by electron microscopy
Thermal tolerance	500°C	500°C	Shrinkage begins gradually at 500°C.
Melting point	>1200°C	>1200°C	
Typical thermal conductivity	0.015 W/mK	0.02 W/mK	
Coefficient of thermal expansion	2.0-4.0 × 10 <sup>-6</sup>	2.0-4.0 × 10 <sup>-6</sup>	Determined using ultrasonic techniques
Poisson's ratio	0.2	0.2	Independent of density
Young's modulus	10 <sup>5</sup> -10 <sup>7</sup> N/m <sup>2</sup>	10 <sup>5</sup> -10 <sup>7</sup> N/m <sup>2</sup>	Insignificant compared to dense silica
Tensile strength	16 kPa	16 kPa	For density of 0.1 g/cm <sup>3</sup>
Fracture toughness	0.8 kPa·m <sup>0.5</sup>	0.8 kPa·m <sup>0.5</sup>	For density of 0.1 g/cm <sup>3</sup>
Index of refraction	1.0-1.05	1.0-1.05	
Dielectric constant	~1.1	~1.1	For density of 0.1 g/cm <sup>3</sup>
Sound velocity	100 m/s	100 m/s	For density of 0.07 g/cm <sup>3</sup>

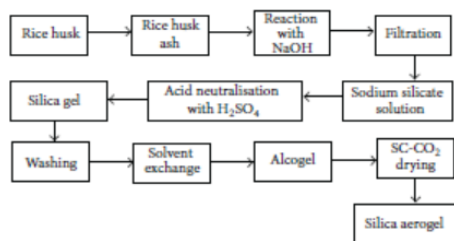


**Figure 2. Schematic procedure of Maerogel preparation from rice husk.**

RHA was used to define alternative strategies in supercritical or ambient conditions. The preparation offered by Tang and Wang has a lower surface area value than that produced by TEOS/supercritical ethanol drying. The aerogel was white rather than translucent.<sup>49</sup> Following that, Li and Wang created a technique using a drying process at atmospheric pressure and a temperature of 40°C.<sup>50</sup>

A little amount of TEOS was added to the hydrosol in this approach, dramatically altering the pore structure and therefore other physical properties. While the density was found to be inversely related to the amount of TEOS applied, the porosity, surface area, pore volume, and average pore size were all shown to be directly proportionate. However, an ideal TEOS level was attained.<sup>51</sup> Leventis et al. created the first metal aerogel in 2009.

It was an iron aerogel made by melting together iron oxide xerogels (ambient-dried aerogels) and resorcinol-formaldehyde aerogels. They were “ferromagnetic and superparamagnetic” materials because they were both magnetic and metallic while also being rich in carbon.<sup>52</sup> At NASA’s Glenn Research Centre in Ohio, a superior polymerized aerogel called as polyimide aerogel has just been developed.<sup>53</sup> By chemically imidizing anhydride-capped polyamic acid oligomers with aromatic triamine in solution, polyimide gels are created. After that, polyimide aerogels are created by supercritically drying the succeeding gels. These modified aerogels exhibit surface areas of 512m<sup>2</sup>/g and densities as low as 0.14 g/cm<sup>3</sup>.<sup>54,55</sup> This novel form of aerogel has a mechanical strength that is 500 times more than that of conventional silica and can offer substantial thermal and acoustic insulation. However, the thermal conductivity is increased by a certain factor because of its monolithic nature.<sup>53</sup>

**Properties of Silica Aerogels**

The density and chemical make-up of an aerogel have a significant impact on its physical characteristics. As a result, different synthesis techniques will produce different usual values for particular characteristics. Table 1 illustrates this. An understanding of the thermal, optical, and mechanical characterizations of silica aerogels has been provided in accordance with the purview of this article.

Thermal Properties - Since the outset, silica aerogels’ thermal conductivity has been the main focus of research. Depending on the intended application, aerogels can be created as monoliths, grains, powders, and films. Monolithic silica aerogels have been employed by NASA in the past for space applications’ thermal insulation.<sup>56</sup> Three heat transfer processes are responsible for the total thermal conductivity (t) of monolithic aerogels: solid conduction via the solid backbone (s), gaseous conduction through the gas molecules in the porous structure (g), and radiation (r).<sup>57</sup> Aerogels’ nanoscale holes allow convection to be disregarded.<sup>58,59</sup>

Because only a small number of silica particles are tortuously linked in a three-dimensional network with many dead ends, the solid structure of aerogels obstructs the flow of heat.<sup>15</sup> According to studies, the lattice structure, connectivity, and composition of an aerogel affect how much heat is

transferred through its solid structure.

The density and particle interconnectivity were used by Lu et al. to calculate the solid thermal conductivity [60]. Bi and Tang et al. offered a more practical equation in which the solid thermal conductivity  $s$  is determined by measuring the sound velocity in the aerogel.<sup>61</sup>

$$\lambda_s = \lambda_0 \frac{\rho}{\rho_0} \frac{\nu}{\nu_0}, \quad (1)$$

Because only a small number of silica particles are tortuously linked in a three-dimensional network with many dead ends, the solid structure of aerogels obstructs the flow of heat.<sup>15</sup> According to studies, the lattice structure, connectivity, and composition of an aerogel affect how much heat is transferred through its solid structure.

The density and particle interconnectivity were used by Lu et al. to calculate the solid thermal conductivity [60]. Bi and Tang et al. offered a more practical equation in which the solid thermal conductivity  $s$  is determined by measuring the sound velocity in the aerogel.<sup>61</sup>

$$\lambda_0 = C_v \nu_0 \frac{\Lambda_0}{3}, \quad (2)$$

where  $C_v$  is the volume specific heat,  $\Lambda_0$  is the solid backbone's mean sound velocity, and  $\Lambda_0$  is the average interatomic distance.

The Knudsen effect, which describes the gaseous conduction in a porous media as a function of the air pressure and the effective pore dimension, governs the heat transfer through the gaseous phase.<sup>60</sup> This is the related equation:

$$\lambda_g = \lambda_{g0} \frac{\Pi}{1 + \beta K_n}, \quad (3)$$

Where

$$K_n = \frac{l_g}{\phi}, \quad (4)$$

$$I_{\text{mean}} = \frac{\kappa_B T}{\sqrt{2}} \pi d_g^2 P_g, \quad (5)$$

where  $K_n$  is the Knudsen number, which is a measure of the thermal conductivity of gas in a porous medium.  $l_g$  is the average free path of the gas molecules,  $\phi$  is the characteristic length of the pores,  $d_g$  is the diameter of the gas molecules,  $\phi$  is the porosity,  $\lambda_{g0}$  is the thermal conductivity in free air,  $\kappa_B$  is the Boltzmann constant,  $T$  is the temperature,  $P_g$  is the gas pressure, and  $\beta$  is a constant particular to the gas in the pores, typically between 1.5 and 2.0.<sup>62</sup>

In silica aerogels, the pressure, pore size, and density are all directly correlated with the gaseous thermal conductivity. In addition, the solid nanoscale structure of aerogels significantly affects the thermal conductivity of gas, especially for pressures between 0.01 and 100 Pa.

Due to their low infrared absorption, aerogels can exhibit significant radiation effects on their total thermal conductivity from low temperatures (below 200C) to high temperatures.<sup>10</sup> Calculations for radiative conductivity can be found in.<sup>60</sup>

$$\lambda_r = \left(\frac{16}{3}\right) n^2 \sigma \frac{T^3}{[e(T)\rho]}, \quad (6)$$

where  $\sigma$  is the Stefan-Boltzmann constant,  $n$  is the mean index of refraction of aerogel,  $T$  is the absolute temperature,  $e(T)$  is the mass specific extinction coefficient, and  $\rho$  is the density of aerogel. It is worthwhile to note that there is an alternative approach to evaluate the effective thermal conductivity of silica aerogel  $\lambda_{\text{eff}}$ . It uses a concept where the heat transfer mechanisms are radiation and a combined solid and gas conduction. The solid and gas thermal conductivity  $\lambda_c$  is developed based on a periodic structure, whilst the radiative conductivity  $\lambda_r$  is calculated using the diffusion approximation theory and the Rosseland equation.<sup>58,64,65</sup> The common techniques to measure the thermal conductivities of silica aerogels are hot-wire probe<sup>69</sup>, hot disk thermal constant analysers<sup>70</sup>, and heat-fluxmeters<sup>71</sup> or using

a laser-flash apparatus.<sup>72</sup> However, in these techniques, the heat distribution across the aerogel under study is not uniform. Zeng et al.<sup>73</sup> suggested a way out where a thin-film heater made of a 10 nm thick gold film can be used to disperse the heat evenly. Table 2 summarizes the different approaches to predict the thermal conductivity of silica aerogels. 3.2. Optical Properties. The transparency and translucency

appearances of aerogels are primarily due to Rayleigh scattering, which occurs when the heterogeneities in the solid gel network are much smaller than the wavelength of visible light.

The amount of light scattered from an aerogel is dependent on these structural inhomogeneities which in turn can be controlled during the supercritical extraction which dictates the spatial arrangements of the gel network. Rayleigh scattering

is inversely proportional to the fourth power of the wavelength, that is, the shorter the wavelength of the light, the more it scatters. Therefore, when an aerogel tile is placed against a dark background, it appears slightly bluish and demonstrates a yellowish coloration when exposed to bright surroundings.<sup>74,75</sup> This second source of light scattering in the visible range is due to micrometer-size imperfections of the external aerogel surface which accounts for the blurry appearance of objects viewed through a piece of aerogel.<sup>76</sup> On the other hand, the scattering efficiency is a function of the size of the scattering center. Thus different wavelengths will scatter with varying magnitudes. Scattering

is observed to be intensified when the size of the scattering center becomes similar to the wavelength of the incident light.<sup>76,77</sup> As the wavelength increases and the spectrum shifts towards the infrared range, scatterings become less significant. This phenomenon permits heat radiation to pass through the aerogel thereby increasing its thermal conductivity.<sup>78</sup> Many times,

the optical properties of aerogels are related with their thermal properties, especially when a transparent thermal insulation system is demanded. A number of studies have been undertaken to optimize the transparency of silica aerogel without sacrificing its thermal conductivity. Danilyuk et al.<sup>79</sup> found that monolithic aerogel prepared using the twostep sol-gel method is more transparent than the one synthesized through the one-step approach. Venkateswara Rao and Pajonk<sup>80</sup> added methyl trimethoxysilane (MTMS) as a coprecursor to produce monolithic durable hydrophobic silica aerogels with high direct optical transmittance and low diffusion of light. Adachi et al.<sup>81</sup> synthesized new tiles of silica aerogels by adding a new chemical solvent, dimethylformamide (DMF), to improve the optical transparency in the refractive index range,  $n = 1.03\text{--}1.07$ . The transmission length exceeded 40mm at 400 nm wavelength which was twice the value obtained in a previous study.<sup>82</sup> Bhagat et al. showed that when low density TEOS-based silica aerogels is prepared using methanol as a solvent in combination with TEOS in a two-step sol-gel process, the optical transmission is improved to some extent.<sup>83</sup> On the contrary, if opacity is preferred, aerogel can be rendered opaque by integrating carbon

or mineral powders into its structure which will absorb the infrared and hence reducing the radiation heat transfer.<sup>84,86</sup> From the early age, transparent silica aerogel has been promoted as a hypervelocity particle capture for outer-space explorations because of its capacity of allowing easy detection of cosmic debris through its framework. Recently, Woignier et al.<sup>87</sup> investigated the effect of TEOS concentration and

the addition of ammonia as a base catalysis on the optical transmission within the visible spectrum. It was found that aerogels with a higher concentration of TEOS have a wider transmission window than that with a lower TEOS concentration which affirms poor transparency in the visible range. When ammonia is added in the aerogel process, the transmission is extraordinarily enhanced in the visible range. Another imperative optical property of silica aerogels is the index of refraction. It has been proven that the index of refraction,  $n$ , increases with increasing density such that

where  $\rho$  ( $\text{kg gm}^{-3}$ ) is the bulk density of aerogel.<sup>1</sup> It can

therefore be anticipated that the refractive index for silica aerogel is very close to one, literally meaning that when light enters an aerogel, there is no reflective losses. A practical application which exploits this property is the Cherenkov detector which necessitates a medium with a refractive index close to one.<sup>88</sup> 3.3. Mechanical Properties. Silica aerogels are known to be characteristically fragile and brittle because of the interparticle connections within the pearl-necklace-like fractal network, making them inapt for load bearing applications. Numerous investigations have been carried out to appreciate and characterize their mechanical properties, as shown in Table 3. Standard methods to characterize the silica aerogel

$$\eta = 1 + 2.1 \times 10^{-4} \rho, \quad (7)$$

mechanically include ultrasonic techniques, three-point bending, and uniaxial compression. The atomic force microscopy (AFM) is now commonly employed because of its capability of measuring the local elastic property of aerogels with only a small loading force. Concurrently, efforts are being

concerted to improve the mechanical strength of aerogels by the addition of a second phase. One approach is through incorporating silica fibres into the aerogels. Tests have indicated that when 10% by weight of these fibres are introduced, the elastic modulus and strength are increased by 85% and 26%, respectively [89]. In addition, the compressive modulus and tensile strength of aerogels can be improved by three and five times correspondingly, if 5% by weight of carbon nanofibres are implemented into the lattice structure [90]. Liquid-phase cross-linking, vapor-phase cross-linking, fibre reinforcing, and reduced bonding can enhance the mechanical properties of aerogel as well [80, 91, 92]. X-aerogels have been proven to improve considerably the fractal properties of native aerogels under both quasi-static [43, 93–97] and high impact

loading conditions [98, 99]. While their strength is superior to silica aerogels, their elasticity and flexibility properties are yet to be tailored for advanced aerospace applications such as structural components and thermal protection for small satellites, spacecraft, planetary vehicles, and habitats. Several cross-linking schemes to mechanically reinforce aerogels have been discussed in details in.<sup>100</sup> It is noteworthy

to state that polymer reinforcement decreases the surface area of the silica aerogel by about half without altering the thermal conductivity radically.<sup>100</sup> Probably, the most notable application of silica aerogel in astronautics is to capture extraterrestrial materials. This is primarily because it does not constitute elements of great cosmochemical significance as well as inorganic contaminants and secondly owing to its grandiosity in trapping particles with high velocities.

Figure 3. mechanical studies on silica aerogel.

Methodology	Author	Analysis	Approach/apparatus
Experimental	Arvidson and Scull [111]	Young's modulus, proportional limit, and yield strength	A concentric, overlapping-cylinder, capacitance extensometer is used to measure the strain
	Gronauer et al. [112]	Young's modulus	Sound velocity measurements
	Woignier and Phalippou [113]	Young's modulus, fracture strength, and toughness	Three-point flexural and three-point bending
	Grow et al. [114]	Young's modulus and Poisson's ratio	Ultrasonic and static compression
	Scherer et al. [115]	Bulk modulus	Mercury porosimetry
	Parmentier and Milstein [89]	Hardness, compression, tension and shear on unreinforced and fiber-reinforced aerogels	Vickers and Knoop hardness test, four-point bending, and a displacement-controlled Instron 1125 testing machine
	Stark et al. [116]	Young's modulus	Atomic force microscopy
	Moner-Girona et al. [117]	Hardness, Young's modulus, and elastic parameter	Microindentation measurements using a NanoTest 550 indenter
	Martin et al. [118]	Young's Modulus	Uniaxial compression and acoustic velocity
	Perin et al. [119]	Elastic modulus and internal friction	Isostatic compression
Numerical	Miner et al. [120]	Young's modulus and nonrecoverable strain for hygroscopic silica aerogel	Low-range compression tester
	Daspeth et al. [121]	Subcritical growth domain in hydrophilic silica aerogel	Double-clawage-drilled-compression test (D/CDC)
	Takahashi et al. [122]	Bending strength	Three-point bending
	Yang et al. [123]	Creep behavior of ceramic fiber-reinforced silica aerogel	Scanning electron microscope
	Hasmy et al. [124]	Wave-vector-dependent scattered intensity	Cubic DLCA fractal structure model
	Rahmani et al. [125]	Densities of states and dynamic structure factors	3D cubic DLCA fractal structure model
	Yang et al. [123]	Creep behavior of ceramic fiber-reinforced silica aerogel	Power-law creep model

Yet, researchers are continually experimenting on this nanomaterial to improve its physical properties to develop a flawless kinetic shock absorber. Most of the time, the modification is made during the synthesis process as the aerogel mechanical characteristics highly depend on its bulk density.<sup>101,102</sup> The mechanical and thermal properties of density-gradient aerogels for outer-space hypervelocity particle capture were analyzed by Du et al. (see Figure 3) [103]. Aerogels with densities ranging from 40 to 175 mg/cm<sup>3</sup> were prepared using a tetraethyl orthosilicate (TEOS) and ethanol-water solution as the precursor and hydrofluoric acid as the catalyst via a

supercritical drying sol-gel process. Layer-by-layer gelation, sol cogelation, and gradient-sol cogelation methods were used to prepare the density-gradient aerogels. The dynamic mechanical test showed that the Young's moduli of the aerogels at -100°C and 25°C tend to decrease with decreasing the density with values from  $4.6 \times 10^5$  to  $1.9 \times 10^5$  Pa and from  $5.0 \times 10^5$  to  $2.1 \times 10^5$  Pa, respectively. The thermal analysis indicated that the thermal diffusion coefficients and the specific heat capacities decrease with decreasing the densities while the thermal conductivities do not change monotonically. One weakness of aerogel as a hypervelocity capture particle

could be its crack propagation which can eventually destroy the entire aerogel lattice when exposed for a long

period of time. This is induced by the syneresis effect which is the continuation of the hydrolysis and condensation reactions after gelling which leads to the gel shrinkage.<sup>87,101</sup> Hwang et al. observed a 10% linear shrinkage caused by syneresis during the gelation and aging procedures.<sup>104</sup> Woignier et al.<sup>87</sup> investigated the influence of the synthesis variables on the shrinkage of aerogel during preparation and delivered a good correlation on the mechanical properties with an aim to acquire an optimized aerogel for outer-space applications. It was revealed that the linear shrinkage decreases with the TEOS concentration and with increasing pH of hydrolysis solution. In addition, both elastic modulus and rupture strength of aerogels rise with a higher concentration of TEOS and hence density. a hypervelocity particle capture compared to traditional dense collector media, including those exposed on the long duration exposure facility (LDEF). The defects in these conventional collectors were their persistent melting, if not complete vaporization, which prevented any projectiles to be adhered. Hence, no analysis was possible. Researchers anticipated that this kinetic energy absorption characteristic to aerogel would boost the discoveries of extraterrestrial

objects in low-Earth orbit.<sup>105</sup>

Soon after, in September 1992, aerogels were sent on the Space Transport System (STS-47) to analyse their ability as a hypervelocity particle capture medium and endurance during launch and reentry. Five thermal insulated end covers were installed on the top of the Shuttle Get Away Special (GAS) payload canisters to hold the Sample Return Experiment (SRE) of capture cells equipped with panels of silica aerogel

with dimensions of 10 cm × 10 cm × 1 cm and densities of the order 20mg/mL. Each GAS SRE provided a net total capture surface area of 0.165m<sup>2</sup>. The aerogels successfully survived the launch and reentry and returned without any apparent damages. Generally, the capability of a hypervelocity particle capture is evaluated by how fast it can decelerate the high velocity impacted particles without destroying the latter while being trapped. At least four large hypervelocity particles were captured during this preliminary mission. Later on, more than two dozens of particles were caught from STS-60 and many from others such GAS canisters.<sup>106</sup> One of them was the orbital debris collection experiment on Mir. Deployed on STS-76 on March 25, 1996, and directed by Langley Research Center, the Mir Environmental Effects Package (MEEP) was equipped with an Orbital Debris Collector (ODC) made up of approximately 0.63m<sup>2</sup> of highly porous low-density (0.02 g/cm<sup>3</sup>) silica aerogel arranged in two identical trays, Tray 1 pointing into the ram direction while Tray 2 in the opposite direction, to collect both manmade and natural hypervelocity particles in the low-Earth orbit. The ODC was then recuperated by STS-86 after 18 months at the Johnson Space Center.

A wide range of impacts, for example, coorbiting flakes, human waste materials, and cosmic dust, were extracted from the aerogel collector to analyse their compositions using SEM-EDS and TEM, and henceforth their potential origins were suggested. Two primary classes of hypervelocity impact features were revealed: long, carrot-shaped tracks and shallow pits with typical length to diameter ( $l/d$ ) of 20–40 and

0.5–5, respectively. The majority were carrot-shaped tracks coming from laboratory impacts, including the presence of trapped projectile residues at their stations while the pits did not contain any measurable residues and laboratory analog due to the high impact velocities causing melting or vaporization of the projectiles. Features of intermediate morphologies between these two boundaries suggested the existence of

a transitional and evolution of sequence. The third group was shallower and irregular impact tracks with aspect ratio,  $l/d < 0.5$ , formed by low-velocity impacts of coorbiting flakes and liquid droplets, all human waste products,

and the result of wastewater dumps. However, aerogel could not yield reliable dynamic data for each particle, including chronological information about the collisions. Nevertheless, the unique ability of aerogel to preserve and trap unmolten residues at relatively high velocities in low-Earth orbit was

confirmed compared to traditional nonporous media; those threshold velocities for vaporization were much smaller than aerogel.<sup>105,107</sup>

The most successful aerogel-related mission that has unveiled many scientific discoveries is probably the Stardust Mission. Launched from the Kennedy Space Center in 1999, the function of the mission was to carry a hypervelocity particle collector which would meet up with a known outer solar system body (Comet 81P/Wild 2) to capture coma samples and interstellar dust to be brought on Earth for laboratory analysis.<sup>108,110</sup> The collector, a “tennis-racket”-shaped metal frame, consisted of two grids facing in opposite direction, each of them containing one hundred and thirty cells of silica aerogel of different volumes (see Figure 4).<sup>127</sup> One grid had cubes of dimensions approximately 4 cm × 2 cm × 3 cm to capture cometary particles, whilst the other grid contained aerogel tiles with dimensions 4 cm × 2 cm × 1 cm to seize interstellar materials.<sup>56</sup> When collection was required, the collector was detached from the protective sample return (SRC) and

exposed. Compared to the missions stated above, the aerogel created for that assignment had a continuous gradient density profile, starting from 10mg/cm<sup>3</sup> at the impact surface to a higher value at the bottom depending on the type of the grid. The maximum densities were 50mg/cm<sup>3</sup> and 20mg/cm<sup>3</sup> for

the cometary grid and interstellar grid, respectively. It was already recognized that the density depends on the ratio of the condensable silica of the solvent used in the aerogel precursor solution. That concept was exploited when the precursor solution for low-density aerogel was steadily mixed with the precursor solution density aerogel while constantly pumping the resultant mixture into a gradient density silica

aerogel.<sup>128</sup> It could be anticipated that other density dependent characteristics such as thermal, optical, acoustic, and dielectric of aerogel would vary as per the gradient profile.<sup>129</sup> The latter would prevent the nanopores of the silica aerogel from being damaged by the microscale particles. When the high-speed particles hit the aerogel, they first bumped into the low-density aerogel and, as they penetrated, the density of the aerogel increased simultaneously slowing them down. The kinetic energy was converted into mechanical and thermal energy, which in the end brought the speed to zero.<sup>130</sup>

In 2004, the Stardust capsule successfully landed in Utah after being retrieved from the SRC to protect samples. Aerogel, despite being brittle, demonstrated its ability to withstand transitions from atmospheric pressure to vacuum of space. The comets were the first materials obtained from a celestial body other than the Moon, revealing high- and low-temperature minerals and unknown organics. Interstellar dusts were also found, but none were recognized. In 2011, a recycle version of Stardust, called Stardust-NExT, was sent to analyze Tempel 1, obtaining high-resolution pictures of the nucleus.

In 2003, the Sample Collection of the Investigation of Mars mission (SCIM) was proposed to collect suspended dust through the upper Martian atmosphere in a silica aerogel collector. The mission was a low-budget and low-risk program, but it was later abandoned due to the technology of Stardust. Other potential aerogel-based collectors include carbon, alumina, titania, germania, zirconia, and niobia.

The Material Exposure and Degradation Experiment (MEDET) was initiated to investigate the effects of the complex low-Earth orbit space environment on material properties and degradation due to contamination while measuring local microparticle flux. Silica aerogel was chosen as a passive detector to capture micrometeoroids and orbital debris particles. A study was conducted to measure the temperatures experienced by hypervelocity particles during their capture in aerogels.

NASA extended its research on aerogel in the field of thermal insulation due to its extremely low conductivity. Silica aerogel was first used as an insulator on the Mars Rover Sojourner in 1997, and was later used in the Mars Exploration Rovers Spirit and Opportunity in 2003. To increase the performance of the silica aerogel as an insulation material, its composition was modified by doping graphite with necessary alteration in the drying process to ensure no cracking and shrinking. The aerogels were then shaped into relatively large panels.

Silica aerogels are being studied for use in space suits to ensure astronaut safety in harsh conditions. The extravehicular mobility unit (EMU) is divided into five layers, including the thermal micrometeoroid garment (TMG), which provides thermal and micrometeoroid protection. The MLI has low thermal conductivity due to radiation heat transfer and interstitial gases on Mars.

Arcypumping, the accumulation of dense air, ice, water, and liquefied air within insulation materials, is a primary concern in spacecraft. Aerogel has been considered as a potential candidate to act as a heat shield in cryogenic systems like liquid-hydrogen tanks and liquid-oxygen feedlines due to its fully breathable and hydrophobic characteristics. Experiments have shown that liquid nitrogen can be prevented from accumulating within the intertank of the

space shuttle by using an insulation system consisting of a bulk-fill aerogel material.

Silica aerogel has been used in various insulation test cryostats at NASA's Kennedy Space Center, with results showing that cryopumping effects were stopped beyond thermal stabilization. This superinsulation material could be used to design lightweight and robust vehicles that ensure safety during operations.

A manned mission to Mars has been proposed, and silica aerogel has been selected to provide thermal insulation for floors, walls, and windows. The concept requires a thin flexible aerogel with low thermal conductivity, making Spaceloft a probable choice.

### Evaluation of Silica Aerogels in Aeronautics

The Federal Aviation Regulations require thermal and acoustical insulation to be provided by the same material while being fire retardant. This applies primarily for the fuselage, with fiberglass batting being the current material. Silica aerogel, a superinsulation material and an acoustic shock-absorber, can be considered as a thermal/acoustical insulator. It can be applied in two modes: as a thin insulative coating to protect uneven substrates from high temperatures, or as flexible lightweight blankets in compartments with high vibration.

Silica aerogel is an excellent firewall compared to existing combustible organic coatings, allowing weight savings and protection of components like pipes, wires, and electronic accessories within the fire zones of an aeroengine. However, the product Pyrogel 6350 has not been commercialized for aeronautical applications.

Acoustics can also be achieved through silica aerogels, as sound waves are significantly absorbed through them, reducing the speed of propagation to 100m/s. Silica aerogel is now acknowledged as a promising material for acoustic matching layers of high-sensitivity airborne ultrasonic transducers for boosting airborne acoustic waves.

However, the main limitation of silica aerogel from commercially integrating into the aviation sector is its high cost. American Airlines claimed to have saved \$422 million in operating costs through fuel savings in 2011. Reducing take-off weight can save about 1 million jet fuel gallons annually.

The leading companies for mass production of silica aerogel are Cabot Corporation and Aspen Aerogels, which produce granules under the Trademark Nanogel and flexible blankets under Cryogels, Pyrogels, and Spaceloft. However, it remains difficult to compensate the price of silica aerogel for other beneficial factors.

### Conclusions

Over 80 years of research have led to the understanding of the synthesis-structure-property relationships of aerogels. They have been commercialized in high-tech areas, with superior capture effectiveness as a kinetic energy absorber and potential as thermal insulation. However, lower thermal conductivity is required for space suits. Silica aerogel fulfills fire retardation requirements in aeroengines, but further study is needed for acoustical applications. Maerogel, an eco-friendly material, is proposed as a promising substitute due to its low cost and comparable properties.

## References

1. J. Fricke and T. Tillotson, "Aerogels: production, characterization, and applications," *Thin Solid Films*, vol. 297, no. 1-2, pp. 212–223, 1997.
2. J. Fricke and A. Emmerling, "Aerogels—recent progress in production techniques and novel applications," *Journal of Sol-Gel Science and Technology*, vol. 13, no. 1–3, pp. 299–303, 1999.
3. M. Schmidt and F. Schwertfeger, "Applications for silica aerogel products," *Journal of Non-Crystalline Solids*, vol. 225, no. 1–3, pp. 364–368, 1998.
4. G. Herrmann, R. Iden, M. Mielke, F. Teich, and B. Ziegler, "On the way to commercial production of silica aerogel," *Journal of Non-Crystalline Solids*, vol. 186, pp. 380–387, 1995.
5. Y. K. Akimov, "Fields of application of aerogels," *Pribory i Tekhnika Eksperimenta*, vol. 46, no. 3, pp. 5–19, 2003.
6. A. C. Pierre and G. M. Pajonk, "Chemistry of aerogels and their applications," *Chemical Reviews*, vol. 102, no. 11, pp. 4243–4265, 2002.
7. C. A. M. Mulder and J. G. Lierop, "Preparation, densification and characterization of autoclave dried SiO<sub>2</sub> gels," in *Aerogels*, J. Fricke, Ed., pp. 68–75, Springer, Berlin, Germany, 1986.
8. L. W. Hrubesh, "Aerogels: the world's lightest solids," *Chemistry and Industry*, no. 24, pp. 824–827, 1990.
9. S. R. Hostler, A. R. Abramson, M. D. Gawryla, S. A. Bandi, and D. A. Schiraldi, "Thermal conductivity of a clay-based aerogel," *International Journal of Heat and Mass Transfer*, vol. 52, no. 3-4, pp. 665–669, 2009.
10. G. Wei, Y. Liu, X. Zhang, F. Yu, and X. Du, "Thermal conductivities study on silica aerogel and its composite insulation materials," *International Journal of Heat and Mass Transfer*, vol. 54, no. 11-12, pp. 2355–2366, 2011.
11. G. Wei, Y. Liu, X. Du, and X. Zhang, "Gaseous conductivity study on silica aerogel and its composite insulation materials," *Journal of Heat Transfer*, vol. 134, no. 4, Article ID 041301, 5 pages, 2012.
12. J.-J. Zhao, Y.-Y. Duan, X.-D. Wang, and B.-X. Wang, "A 3-D numerical heat transfer model for silica aerogels based on the porous secondary nanoparticle aggregate structure," *Journal of Non-Crystalline Solids*, vol. 358, no. 10, pp. 1287–1297, 2012.
13. J.-J. Zhao, Y.-Y. Duan, X.-D. Wang, and B.-X. Wang, "An analytical model for combined radiative and conductive heat transfer in fiber-loaded silica aerogels," *Journal of Non-Crystalline Solids*, vol. 358, no. 10, pp. 1303–1312, 2012.
14. S. S. Kistler, "Coherent expanded aerogels and jellies," *Nature*, vol. 127, no. 3211, p. 741, 1931.
15. S. S. Kistler, "Coherent expanded aerogels," *Journal of Physical Chemistry*, vol. 36, no. 1, pp. 52–64, 1932.
16. S. S. Kistler, "The relation between heat conductivity and structure in silica aerogel," *Journal of Physical Chemistry*, vol. 39, no. 1, pp. 79–85, 1935.
17. Stardust. NASA, January 2013, <http://stardust.jpl.nasa.gov/photo/aerogel.html>.
18. S. S. Kistler and A. G. Caldwell, "Thermal conductivity of silica aerogel," *Industrial & Engineering Chemistry*, vol. 26, pp. 658–662, 1934.
19. C. E. Carraher Jr., "General topics," *Polymer News*, vol. 30, no. 2, pp. 62–64, 2005.
20. G. M. Pajonk, "Some applications of silica aerogels," *Colloid and Polymer Science*, vol. 281, no. 7, pp. 637–651, 2003.
21. S. J. Teichner and G. A. Nicolao, "Method of preparing inorganicaerogels," US patent no. 3,672,833, 1972.
22. S. J. Teichner, G. A. Nicolaon, M. A. Vicarini, and G. E. E. Gardes, "Inorganic oxide aerogels," *Advances in Colloid and Interface Science*, vol. 5, no. 3, pp. 245–273, 1976.
23. G. Poelz and R. Riethmüller, "Preparation of silica aerogel for Cherenkov counters," *Nuclear Instruments and Methods*, vol. 195, no. 3, pp. 491–503, 1982.
24. Airglass AB, January 2013, <http://www.airglass.se/>.
25. P. H. Tewari and A. J. Hunt, "Process for forming transparent aerogel insulating arrays," US patent no. 4,610,863, 1986.
26. P. H. Tewari, A. J. Hunt, and K. D. Lofftus, "Ambient-temperature supercritical drying of transparent silica aerogels," *Materials Letters*, vol. 3, no. 9-10, pp. 363–367, 1985.
27. T. Woignier and J. Phalippou, "Skeletal density of silica aerogels," *Journal of Non-Crystalline Solids*, vol. 93, no. 1, pp. 17–21, 1987.
28. R. W. Pekala, "Organic aerogels from the polycondensation of resorcinol with formaldehyde," *Journal of Materials Science*, vol. 24, no. 9, pp. 3221–3227, 1989.
29. T. M. Tillotson and L. W. Hrubesh, "Transparent ultralow-density silica aerogels prepared by a two-step sol-gel process," *Journal of Non-Crystalline Solids*, vol. 145, pp. 44–50, 1992.
30. S. T. Mayer, R. W. Pekala, and J. L. Kaschmitter, "Theaerocapacitor: an electrochemical double-layer energy-storage device," *Journal of the Electrochemical Society*, vol. 140, no. 2, pp. 446–451, 1993.

31. R. W. Pekala, S. T. Mayer, J. L. Kaschmitter, and F. M. Kong, "Carbon aerogels: an update on structure, properties, and applications," in *Sol-Gel Processing and Applications*, Y. A. Attia, Ed., pp. 369–377, Springer, Berlin, Germany, 1994.
32. D. M. Smith, R. Deshpande, and C. J. Brinker, "Preparation of low-density aerogels at ambient pressure," in *Better Ceramics through Chemistry V*, M. J. Hampden-Smith, W. G. Klemperer, and C. J. Brinker, Eds., vol. 271 of *MRS Proceedings*, pp. 567–572, 1992.
33. S. S. Prakash, C. J. Brinker, A. J. Hurd, and S. M. Rao, "Silica aerogel films prepared at ambient pressure by using surface derivatization to induce reversible drying shrinkage," *Nature*, vol. 374, pp. 439–443, 1995.
34. F. Shi, L. Wang, and J. Liu, "Synthesis and characterization of silica aerogels by a novel fast ambient pressure drying process," *Materials Letters*, vol. 60, no. 29-30, pp. 3718–3722, 2006.
35. T.-Y. Wei, T.-F. Chang, S.-Y. Lu, and Y.-C. Chang, "Preparation of monolithic silica aerogel of low thermal conductivity by ambient pressure drying," *Journal of the American Ceramic Society*, vol. 90, no. 7, pp. 2003–2007, 2007.
36. S. D. Bhagat, Y.-H. Kim, K.-H. Suh, Y.-S. Ahn, J.-G. Yeo, and J.-H. Han, "Superhydrophobic silica aerogel powders with simultaneous surface modification, solvent exchange and sodium ion removal from hydrogels," *Microporous and Mesoporous Materials*, vol. 112, no. 1–3, pp. 504–509, 2008.
37. P. M. Shewale, A. Venkateswara Rao, A. Parvathy Rao, and S. D. Bhagat, "Synthesis of transparent silica aerogels with low density and better hydrophobicity by controlled sol-gel route and subsequent atmospheric pressure drying," *Journal of Sol-Gel Science and Technology*, vol. 49, no. 3, pp. 285–292, 2009.
38. S.-W. Hwang, T.-Y. Kim, and S.-H. Hyun, "Effect of surface modification conditions on the synthesis of mesoporous crack-free silica aerogel monoliths from water glass via ambient drying," *Microporous and Mesoporous Materials*, vol. 130, no. 1–3, pp. 295–302, 2010.
39. S.-K. Kang and S.-Y. Choi, "Synthesis of low-density silica gel at ambient pressure: effect of heat treatment," *Journal of Materials Science*, vol. 35, no. 19, pp. 4971–4976, 2000.
40. J. F. Poco, P. R. Coronado, R. W. Pekala, and L. W. Hrubesh, "A rapid supercritical extraction process for the production of silica aerogels," in *Microporous and Macroporous Materials*, J. S. Beck, D. R. Corbin, M. E. Davis, L. E. Iton, and R. F. Lobo, Eds., vol. 431 of *MRS Proceedings*, pp. 297–302, 1996.
41. T. B. Roth, A. M. Anderson, and M. K. Carroll, "Analysis of a rapid supercritical extraction aerogel fabrication process: prediction of thermodynamic conditions during processing," *Journal of Non-Crystalline Solids*, vol. 354, no. 31, pp. 3685–3693, 2008.
42. A. E. Gash, T. M. Tillotson, J. H. Satcher Jr., L. W. Hrubesh, and R. L. Simpson, "New sol-gel synthetic route to transition and main-group metal oxide aerogels using inorganic salt precursors," *Journal of Non-Crystalline Solids*, vol. 285, no. 1–3, pp. 22–28, 2001.
43. N. Leventis, C. Sotiriou-Leventis, G. Zhang, and A.-M. M. Rawashdeh, "Nanoengineering strong silica aerogels," *Nano Letters*, vol. 2, no. 9, pp. 957–960, 2002.
44. L. Leventis, S. Mulik, and C. Sotiriou-Leventis, "Crosslinking 3D assemblies of silica nanoparticles (aerogels) by surface-initiated free radical polymerization of styrene and methylmethacrylate," *Polymer Preprints*, vol. 48, pp. 950–951, 2007.
45. J. L. Mohanan, I. U. Arachchige, and S. L. Brock, "Porous semiconductor chalcogenide aerogels," *Science*, vol. 307, no. 5708, pp. 397–400, 2005.
46. B. C. Tappan, M. H. Huynh, M. A. Hiskey et al., "Ultralow-density nanostructured metal foams: combustion synthesis, morphology, and composition," *Journal of the American Chemical Society*, vol. 128, no. 20, pp. 6589–6594, 2006.
47. M. B. Bryning, D. E. Milkie, M. F. Islam, L. A. Hough, J. M. Kikkawa, and A. G. Yodh, "Carbon nanotube aerogels," *Advanced Materials*, vol. 19, no. 5, pp. 661–664, 2007.
48. H. Halimaton, "Silica aerogels," US patent no. 20070276051A1, 2007.
49. Q. Tang and T. Wang, "Preparation of silica aerogel from rice hull ash by supercritical carbon dioxide drying," *The Journal of Supercritical Fluids*, vol. 35, no. 1, pp. 91–94, 2005.
50. T. Li and T. Wang, "Preparation of silica aerogel from rice hull ash by drying at atmospheric pressure," *Materials Chemistry and Physics*, vol. 112, no. 2, pp. 398–401, 2008.
51. A. Tadjarodi, M. Haghverdi, and V. Mohammadi, "Preparation and characterization of nano-porous silica aerogel from rice husk ash by drying at atmospheric pressure," *Materials Research Bulletin*, vol. 47, no. 9, pp. 2584–2589, 2012.
52. N. Leventis, N. Chandrasekaran, C. Sotiriou-Leventis, and A. Mumtaz, "Smelting in the age of nano: iron aerogels," *Journal of Materials Chemistry*, vol. 19, no. 1, pp. 63–65, 2009.
53. M. A. Meador and H. Guo, "Polyimide aerogel thin films," Patent application LEW-18864-1, 2012.
54. H. Guo, M. A. B. Meador, L. McCorkle et al., "Tailoring properties of cross-linked polyimide aerogels for better moisture resistance, flexibility, and strength," *ACS Applied Materials & Interfaces*, vol. 4, no. 10, pp. 5422–5429, 2012.
55. M. A. B. Meador, E. J. Malow, R. Silva et al., "Mechanically

- strong, flexible polyimide aerogels cross-linked with aromatic triamine," *ACS Applied Materials & Interfaces*, vol. 4, no. 2, pp. 536–544, 2012.
56. S. M. Jones, "Aerogel: space exploration applications," *Journal of Sol-Gel Science and Technology*, vol. 40, no. 2-3, pp. 351–357, 2006.
57. J. Fricke, X. Lu, P.Wang, D. B`uttner, and U. Heinemann, "Optimization of monolithic silica aerogel insulants," *International Journal of Heat and Mass Transfer*, vol. 35, no. 9, pp. 2305–2309, 1992.
58. J. J. Zhao, Y. Y. Duan, X. D.Wang, and B. X.Wang, "Radiative properties and heat transfer characteristics of fiber-loaded silica aerogel composites for thermal insulation," *International Journal of Heat and Mass Transfer*, vol. 55, no. 19-20, pp. 5196–5204, 2012.
59. G. R. Cunnington, S. C. Lee, and S. M.White, "Radiative properties of fiber-reinforced aerogel: theory versus experiment," *Journal of Thermophysics and Heat Transfer*, vol. 12, no. 1, pp. 17–22, 1998.
60. X. Lu, R. Caps, J. Fricke, C. T. Alviso, and R. W. Pekala, "Correlation between structure and thermal conductivity of organic aerogels," *Journal of Non-Crystalline Solids*, vol. 188, no. 3, pp. 226–234, 1995.
61. C. Bi and G. H. Tang, "Effective thermal conductivity of the solid backbone of aerogel," *International Journal of Heat and Mass Transfer*, vol. 64, pp. 452–456, 2013.
62. O.-J. Lee, K.-H. Lee, T. Jin Yim, S. Young Kim, and K.-P. Yoo, "Determination of mesopore size of aerogels from thermal conductivity measurements," *Journal of Non-Crystalline Solids*, vol. 298, no. 2-3, pp. 287–292, 2002.
63. Y. Duan, J. Lin, X. Wang, and J. Zhao, "Analysis of gaseous thermal conductivity models for silica aerogels," *CIESC Journal*, vol. 63, pp. 54–58, 2012.
64. G. Wei, Y. Liu, X. Zhang, and X. Du, "Radiative heat transfer study on silica aerogel and its composite insulation materials," *Journal of Non-Crystalline Solids*, vol. 362, pp. 231–236, 2013.
65. G. Lu, X.-D. Wang, Y.-Y. Duan, and X.-W. Li, "Effects of nonideal structures and high temperatures on the insulation properties of aerogel-based composite materials," *Journal of Non-Crystalline Solids*, vol. 357, no. 22-23, pp. 3822–3829, 2011.
66. Z. Jun-Jie, D. Yuan-Yuan, W. Xiao-Dong, and W. Bu-Xuan, "Experimental and analytical analyses of the thermal conductivities and high-temperature characteristics of silica aerogels based on microstructures," *Journal of Physics D*, vol. 46, no. 1, Article ID 015304, 2013.
67. J.Wang, J.Kuhn, and X. Lu, "Monolithic silica aerogel insulation doped with TiO<sub>2</sub> powder and ceramic fibers," *Journal of Non-Crystalline Solids*, vol. 186, pp. 296–300, 1995.
68. S. Spagnol, B. Lartigue, A. Trombe, and V. Gibiat, "Modeling of thermal conduction in granular silica aerogels," *Journal of Sol-Gel Science and Technology*, vol. 48, no. 1-2, pp. 40–46, 2008.
69. D.Haranath, G. M. Pajonk, P.B.Wagh, and A.V.Rao, "Effect of sol-gel processing parameters on thermal properties of silica aerogels," *Materials Chemistry and Physics*, vol. 49, no. 2, pp. 129–134, 1997.
70. G.-S. Kim and S.-H.Hyun, "Synthesis of window glazing coated with silica aerogel films via ambient drying," *Journal of Non-Crystalline Solids*, vol. 320, no. 1–3, pp. 125–132, 2003.
71. J. F.Poco, J. H. Satcher Jr., and L.W. Hrubesh, "Synthesis of high porosity, monolithic alumina aerogels," *Journal of Non-Crystalline Solids*, vol. 285, no. 1–3, pp. 57–63, 2001.
72. V. Bock, O. Nilsson, J. Blumm, and J. Fricke, "Thermal properties of carbon aerogels," *Journal of Non-Crystalline Solids*, vol. 185, no. 3, pp. 233–239, 1995.
73. J. S. Q. Zeng, P. C. Stevens, A. J. Hunt, R. Grief, and D. Lee, "Thin-film-heater thermal conductivity apparatus and measurement of thermal conductivity of silica aerogel," *International Journal of Heat and Mass Transfer*, vol. 39, no. 11, pp. 2311–2317, 1996.
74. W.C.WanqingCao and A. J.Hunt, "Improving the visible transparency of silica aerogels," *Journal of Non-Crystalline Solids*, vol. 176, no. 1, pp. 18–25, 1994.
75. Q. Zhu, Y. Li, and Z. Qiu, "Research progress on aerogels as transparent insulation materials," in *Challenges of Power Engineering and Environment*, K. Cen, Y. Chi, and F.Wang, Eds., pp. 1117–1121, Springer, Berlin, Germany, 2007.
76. A. Emmerling, R. Petricevic, A. Beck, P.Wang, H. Scheller, and J. Fricke, "Relationship between optical transparency and nanostructural features of silica aerogels," *Journal of Non-Crystalline Solids*, vol. 185, no. 3, pp. 240–248, 1995.
77. M. Reim, G. Reichenauer, W. K`orner et al., "Silica-aerogel granulate—structural, optical and thermal properties," *Journal of Non-Crystalline Solids*, vol. 350, pp. 358–363, 2004.
78. A. J. Hunt, "Light scattering for aerogel characterization," *Journal of Non-Crystalline Solids*, vol. 225, no. 1–3, pp. 303–306, 1998.
79. A. F. Danilyuk, E. A. Kravchenko, A. G. Okunev, A. P. Onuchin, and S. A. Shaurman, "Synthesis of aerogel tiles with high light scattering length," *Nuclear Instruments and Methods in Physics Research A*, vol. 433, no. 1, pp. 406–407, 1999.
80. A. Venkateswara Rao and G. M. Pajonk, "Effect of methyltrimethoxysilane as a co-precursor on the optical properties of silica aerogels," *Journal of Non-Crystalline Solids*, vol. 285, no. 1–3, pp. 202–209, 2001.
81. I.Adachi, Y. Ishii, H. Kawai, A. Kuratani, and M. Tabata,

- "Study of a silica aerogel for a Cherenkov radiator," *Nuclear Instruments and Methods in Physics Research A*, vol. 595, no. 1, pp. 180–182, 2008.
82. I. Adachi, S. Fratina, T. Fukushima et al., "Study of highly transparent silica aerogel as a RICH radiator," *Nuclear Instruments and Methods in Physics Research A*, vol. 553, no. 1-2, pp. 146–151, 2005.
  83. S. D. Bhagat, H. Hirashima, and A. Venkateswara Rao, "Low density TEOS based silica aerogels using methanol solvent," *Journal of Materials Science*, vol. 42, no. 9, pp. 3207–3214, 2007.
  84. M. A. Worsley, J. H. Satcher, and T. F. Baumann, "Enhanced thermal transport in carbon aerogel nanocomposites containing double-walled carbon nanotubes," *Journal of Applied Physics*, vol. 105, no. 8, Article ID 084316, 2009.
  85. D. Lee, P. C. Stevens, S. Q. Zeng, and A. J. Hunt, "Thermal characterization of carbon-opacified silica aerogels," *Journal of Non-Crystalline Solids*, vol. 186, pp. 285–290, 1995.
  86. J. Kuhn, T. Gleissner, M. C. Arduini-Schuster, S. Korder, and J. Fricke, "Integration of mineral powders into SiO<sub>2</sub> aerogels," *Journal of Non-Crystalline Solids*, vol. 186, pp. 291–295, 1995.
  87. T. Woignier, L. Duffours, P. Colombel, and C. Durin, "Aerogels materials as space debris collectors," *Advances in Materials Science and Engineering*, vol. 2013, Article ID 484153, 6 pages, 2013.
  88. T. Sumiyoshi, I. Adachi, R. Enomoto et al., "Silica aerogels in high energy physics," *Journal of Non-Crystalline Solids*, vol. 225, no. 1–3, pp. 369–374, 1998.
  89. K. E. Parmenter and F. Milstein, "Mechanical properties of silica aerogels," *Journal of Non-Crystalline Solids*, vol. 223, no. 3, pp. 179–189, 1998.
  90. M. A. B. Meador, S. L. Vivod, L. McCorkle et al., "Reinforcing polymer cross-linked aerogels with carbon nanofibers," *Journal of Materials Chemistry*, vol. 18, no. 16, pp. 1843–1852, 2008.
  91. A. V. Rao, M. M. Kulkarni, D. P. Amalnerkar, and T. Seth, "Surface chemical modification of silica aerogels using various alkylalkoxy/chloro silanes," *Applied Surface Science*, vol. 206, no. 1–4, pp. 262–270, 2003.
  92. A. V. Rao, G. M. Pajonk, S. D. Bhagat, and P. Barbooux, "Comparative studies on the surface chemical modification of silica aerogels based on various organosilane compounds of the type R<sub>n</sub>SiX<sub>4-n</sub>," *Journal of Non-Crystalline Solids*, vol. 350, pp. 216–223, 2004.
  93. G. Zhang, A. Dass, A.-M. M. Rawashdeh et al., "Isocyanate crosslinked silica aerogel monoliths: preparation and characterization," *Journal of Non-Crystalline Solids*, vol. 350, pp. 152–164, 2004.
  94. N. Leventis, "Three-dimensional core-shell superstructures: mechanically strong aerogels," *Accounts of Chemical Research*, vol. 40, no. 9, pp. 874–884, 2007.
  95. M. A. B. Meador, L. A. Capadona, L. McCorkle, D. S. Papadopoulos, and N. Leventis, "Structure-property relationships in porous 3D nanostructures as a function of preparation conditions: isocyanate cross-linked silica aerogels," *Chemistry of Materials*, vol. 19, no. 9, pp. 2247–2260, 2007.
  96. M. A. B. Meador, E. F. Fabrizio, F. Ilhan et al., "Cross-linking amine-modified silica aerogels with epoxies: mechanically strong lightweight porous materials," *Chemistry of Materials*, vol. 17, no. 5, pp. 1085–1098, 2005.
  97. N. Leventis, S. Mulik, X. Wang et al., "Polymer nano-encapsulation of templated mesoporous silica monoliths with improved mechanical properties," *Journal of Non-Crystalline Solids*, vol. 354, no. 2–9, pp. 632–644, 2008.
  98. H. Luo, G. Churu, E. F. Fabrizio et al., "Synthesis and characterization of the physical, chemical and mechanical properties of isocyanate-crosslinked vanadia aerogels," *Journal of Sol-Gel Science and Technology*, vol. 48, no. 1-2, pp. 113–134, 2008.
  100. H. Luo, H. Lu, and N. Leventis, "The compressive behavior of isocyanate-crosslinked silica aerogel at high strain rates," *Mechanics of Time-Dependent Materials*, vol. 10, no. 2, pp. 83–111, 2006.
  101. J. P. Randall, M. A. B. Meador, and S. C. Jana, "Tailoring mechanical properties of aerogels for aerospace applications," *ACS Applied Materials & Interfaces*, vol. 3, no. 3, pp. 613–626, 2011.
  102. P. Etienne, J. Phalippou, T. Woignier, and A. Alaoui, "Slow crack growth in aerogels," *Journal of Non-Crystalline Solids*, vol. 188, no. 1-2, pp. 19–26, 1995.
  103. T. Woignier, F. Despetis, A. Alaoui, P. Etienne, and J. Phalippou, "Mechanical properties of gel-derived materials," *Journal of Sol-Gel Science and Technology*, vol. 19, no. 1–3, pp. 163–169, 2000.
  104. A. Du, B. Zhou, J.-Y. Gui et al., "Thermal and mechanical properties of density-gradient aerogels for outer-space hypervelocity particle capture," *Acta Physico-Chimica Sinica*, vol. 28, no. 5, pp. 1189–1196, 2012.
  105. S.-W. Hwang, H.-H. Jung, S.-H. Hyun, and Y.-S. Ahn, "Effective preparation of crack-free silica aerogels via ambient drying," *Journal of Sol-Gel Science and Technology*, vol. 41, no. 2, pp. 139–146, 2007.
  106. F. Hoerz, G. Cress, M. Zolensky, T. H. See, R. P. Bernhard, and J. L. Warren, "Optical analysis of impact features in aerogel from the orbital debris collection experiment on the MIR station," *NASA TM-1999-209372*, 1999.
  107. P. Tsou, "Silica aerogel captures cosmic dust intact,"

- Journal of Non-Crystalline Solids, vol. 186, pp. 415–427, 1995.
108. F. H<sup>o</sup>rz, M. E. Zolensky, R. P. Bernhard, T. H. See, and J. L. Warren, "Impact features and projectile residues in aerogel exposed on Mir," *Icarus*, vol. 147, no. 2, pp. 559–579, 2000.
109. H. A. Ishii, J. P. Bradley, Z. R. Dai et al., "Comparison of comet 81P/Wild 2 dust with interplanetary dust from comets," *Science*, vol. 319, no. 5862, pp. 447–450, 2008.
110. D. E. Brownlee, P. Tsou, K. L. Atkins et al., "Stardust: finessing expensive cometary sample returns," *Acta Astronautica*, vol. 39, no. 1–4, pp. 51–60, 1996.
111. D. E. Brownlee, P. Tsou, J. D. Anderson et al., "Stardust: comet and interstellar dust sample return mission," *Journal of Geophysical Research E*, vol. 108, no. 10, pp. 1–15, 2003.
112. J. M. Arvidson and L. L. Scull, "Compressive properties of silica aerogel at 295, 76, and 20 K," in *Advances in Cryogenic Engineering Materials*, R. P. Reed and A. F. Clark, Eds., pp. 243–250, Springer, Berlin, Germany, 1986.
113. M. Gronauer, A. Kadur, and J. Fricke, "Mechanical and acoustic properties of silica aerogel," in *Aerogels*, J. Fricke, Ed., pp. 167–173, Springer, Berlin, Germany, 1986.
114. T. Woignier and J. Phalippou, "The aerogel glass conversion," *Revue de Physique Appliquée*, vol. 24, pp. 179–184, 1989.
115. J. Gross, G. Reichenauer, and J. Fricke, "Mechanical properties of SiO<sub>2</sub> aerogels," *Journal of Physics D*, vol. 21, no. 9, pp. 1447–1451, 1988.
116. G. W. Scherer, D. M. Smith, X. Qiu, and J. M. Anderson, "Compression of aerogels," *Journal of Non-Crystalline Solids*, vol. 186, pp. 316–320, 1995.
117. R. W. Stark, T. Drobek, M. Weth, J. Fricke, and W. M. Heckl, "Determination of elastic properties of single aerogel powder particles with the AFM," *Ultramicroscopy*, vol. 75, no. 3, pp. 161–169, 1998.
118. M. Moner-Girona, E. Mart<sup>í</sup>nez, A. Roig, J. Esteve, and E. Molins, "Mechanical properties of silica aerogels measured by microindentation: influence of sol-gel processing parameters and carbon addition," *Journal of Non-Crystalline Solids*, vol. 285, no. 1–3, pp. 244–250, 2001.
119. J. Martin, B. Hosticka, C. Lattimer, and P. M. Norris, "Mechanical and acoustical properties as a function of PEG concentration in macroporous silica gels," *Journal of Non-Crystalline Solids*, vol. 285, no. 1–3, pp. 222–229, 2001.
120. L. Perin, A. Faivre, S. Calas-Etienne, and T. Woignier, "Nanostructural damage associated with isostatic compression of silica aerogels," *Journal of Non-Crystalline Solids*, vol. 333, no. 1, pp. 68–73, 2004.
121. M. R. Miner, B. Hosticka, and P. M. Norris, "The effects of ambient humidity on the mechanical properties and surface chemistry of hygroscopic silica aerogel," *Journal of Non-Crystalline Solids*, vol. 350, pp. 285–289, 2004.
122. F. Despetis, P. Etienne, and S. Etienne-Calas, "Subcritical crack growth in silica aerogel," *Journal of Non-Crystalline Solids*, vol. 344, no. 1–2, pp. 22–25, 2004.
123. R. Takahashi, S. Sato, T. Sodesawa, T. Goto, K. Matsutani, and N. Mikami, "Bending strength of silica gel with bimodal pores: effect of variation in mesopore structure," *Materials Research Bulletin*, vol. 40, no. 7, pp. 1148–1156, 2005.
124. X. Yang, Y. Sun, and D. Shi, "Experimental investigation and modeling of the creep behavior of ceramic fiber-reinforced SiO<sub>2</sub> aerogel," *Journal of Non-Crystalline Solids*, vol. 358, no. 3, pp. 519–524, 2012.
125. A. Hasmy, M. Foret, E. Anglaret, J. Pelous, R. Vacher, and R. Jullien, "Small-angle neutron scattering of aerogels: simulations and experiments," *Journal of Non-Crystalline Solids*, vol. 186, pp. 118–130, 1995.
126. A. Rahmani, P. Jund, C. Benoit, and R. Jullien, "Numerical study of the dynamic properties of silica aerogels," *Journal of Physics: Condensed Matter*, vol. 13, no. 23, pp. 5413–5426, 2001.
127. Alibaba, January 2013, <http://www.alibaba.com/>.
128. Stardust. NASA, January 2013, <http://stardust.jpl.nasa.gov/tech/aerogel.html>.
- J.-Y. Gui, B. Zhou, Y.-H. Zhong, A. Du, and J. Shen, "Fabrication of gradient density SiO<sub>2</sub> aerogel," *Journal of Sol-Gel Science and Technology*, vol. 58, no. 2, pp. 470–475, 2011.
129. S. M. Jones, "A method for producing gradient density aerogel," *Journal of Sol-Gel Science and Technology*, vol. 44, no. 3, pp. 255–258, 2007.
130. G. Dom<sup>í</sup>nguez, A. J. Westphal, S. M. Jones, and M. L. F. Phillips, "Energy loss and impact cratering in aerogels: theory and experiment," *Icarus*, vol. 172, no. 2, pp. 613–624, 2004.
131. H. A. Ishii, G. A. Graham, A. T. Kearsley, P. G. Grant, C. J. Snead, and J. P. Bradley, "Rapid extraction of dust impact tracks from silica aerogel by ultrasonic microblades," *Meteoritics and Planetary Science*, vol. 40, no. 11, pp. 1741–1747, 2005.
132. G. J. Flynn, P. Bleuett, J. Borg et al., "Elemental compositions of comet 81P/wild 2 samples collected by stardust," *Science*, vol. 314, no. 5806, pp. 1731–1735, 2006.
133. S. A. Sandford, J. Al<sup>í</sup>eon, C. M. O. Alexander et al., "Organics captured from comet 81P/wild 2 by the stardust spacecraft," *Science*, vol. 314, no. 5806, pp.

- 1720–1724, 2006.
134. M. E. Zolensky, T. J. Zega, H. Yano et al., “Mineralogy and petrology of comet 81P/Wild 2 nucleus samples,” *Science*, vol. 314, no. 5806, pp. 1735–1739, 2006.
135. K. D. McKeegan, J. Al’eon, J. Bradley et al., “Isotopic compositions of cometary matter returned by stardust,” *Science*, vol. 314, no. 5806, pp. 1724–1728, 2006.
136. M. F. A’Hearn, M. J. S. Belton, W. A. Delamere et al., “Deep impact: excavating comet tempel 1,” *Science*, vol. 310, no. 5746, pp. 258–264, 2005.
137. T. E. Economou, S. F. Green, D. E. Brownlee, and B. C. Clark, “Dust flux monitor instrument measurements during Stardust- NExT Flyby of Comet 9P/Tempel 1,” *Icarus*, vol. 222, no. 2, pp. 526–539, 2013.
138. J. Veverka, K. Klaasen, M. A’Hearn et al., “Return to Comet Tempel 1: overview of Stardust-NExT results,” *Icarus*, vol. 222, no. 2, pp. 424–435, 2013.
139. L. A. Leshin, A. Yen, J. Bomba et al., “Sample collection for investigation of mars (SCIM): An early mars sample return mission through the mars scout program,” in *Proceedings of the 33rd Annual Lunar and Planetary Science Conference*, Lunar Planetary Institute, 2002, abstract no. 1721.
140. L. A. Leshin, B. C. Clark, L. Forney et al., “Scientific benefit of a mars dust sample capture and earth return with SCIM,” in *Proceedings of the 34th Annual Lunar and Planetary Science Conference*, Lunar Planetary Institute, 2003, abstract no. 1288.
- 142.